Cell PRESS

Chemistry & Biology
Article

An Iterative, Bimodular Nonribosomal Peptide Synthetase that Converts Anthranilate and Tryptophan into Tetracyclic Asperlicins

Xue Gao,[1] Wei Jiang,[3] Gonzalo Jiménez-Osés,[2] Moon Seok Choi,[1] Kendall N. Houk,[2] Yi Tang,[1,2,*] and Christopher T. Walsh[3,*]
[1]Department of Chemical and Biomolecular Engineering
[2]Department of Chemistry and Biochemistry
University of California, Los Angeles, 420 Westwood Plaza, Los Angeles, CA 90095, USA
[3]Department of Biological Chemistry and Molecular Pharmacology, Harvard Medical School, 240 Longwood Avenue, Boston, MA 02115, USA
*Correspondence: yitang@ucla.edu (Y.T.), christopher_walsh@hms.harvard.edu (C.T.W.)
http://dx.doi.org/10.1016/j.chembiol.2013.04.019

SUMMARY

The bimodular 276 kDa nonribosomal peptide synthetase AspA from *Aspergillus alliaceus*, heterologously expressed in *Saccharomyces cerevisiae*, converts tryptophan and two molecules of the aromatic β-amino acid anthranilate (Ant) into a pair of tetracyclic peptidyl alkaloids asperlicin C and D in a ratio of 10:1. The first module of AspA activates and processes two molecules of Ant iteratively to generate a tethered Ant-Ant-Trp-*S*-enzyme intermediate on module two. Release is postulated to involve tandem cyclizations, in which the first step is the macrocyclization of the linear tripeptidyl-S-enzyme, by the terminal condensation (C_T) domain to generate the regioisomeric tetracyclic asperlicin scaffolds. Computational analysis of the transannular cyclization of the 11-membered macrocyclic intermediate shows that asperlicin C is the kinetically favored product due to the high stability of a conformation resembling the transition state for cyclization, while asperlicin D is thermodynamically more stable.

INTRODUCTION

The *aspergilli* are prolific producers of polyketide and nonribosomal peptide natural products, some of which appear to be constitutive while others are conditional metabolites (Bok et al., 2006; Sanchez et al., 2012). The peptidyl alkaloids represent a prevalent class, typified by fused ring scaffolds with rigidified frameworks and extended molecular architectures (Chang et al., 1985; Gao et al., 2011; Karwowski et al., 1993; Liesch et al., 1988; Takahashi et al., 1995). These are assembled efficiently by short nonribosomal peptide synthetase (NRPS) assembly lines (Finking and Marahiel, 2004; Sattely et al., 2008) and then further modified by postassembly line tailoring enzymes that can add electrophilic acyl, prenyl, and oxygen functionalities in scaffold maturation events (Ames et al., 2010; Haynes et al., 2011; Yin et al., 2009). We have recently examined the chemical logic and enzymatic machinery for assembly of *Aspergillus* signature metabolites such as fumiquinazolines from *Aspergillus fumigatus* (Ames et al., 2011; Ames and Walsh, 2010), ardeemins from *Aspergillus fischeri* (Haynes et al., 2013), and asperlicins from *Aspergillus alliaceus* (Haynes et al., 2012), which are notable for utilizing the nonproteinogenic β-amino acid anthranilate (Ant) as a chain-initiating building block (Walsh et al., 2012, 2013; Figure 1A). The tricyclic scaffold of fumiquinazoline F is assembled from Ant, L-tryptophan (L-Trp), and L-alanine (L-Ala) by trimodular NRPS enzymatic action (Gao et al., 2012).

In analogy, two molecules of Ant and one L-Trp building block are processed to the tetracyclic isomers asperlicin C and asperlicin D (Haynes et al., 2012). Surprisingly, the AspA NRPS presumed to assemble these asperlicin isomeric frameworks is predicted to be bimodular, not trimodular, with bioinformatic identification and subsequent genetic deletion analysis in the producer (Haynes et al., 2012). This suggests either an unusual iterative action in Ant activation or a possible third module encoded elsewhere in the *A. alliaceus* genome acting in *trans* with AspA. In this work, we have expressed the 276 kDa AspA protein in *Saccharomyces cerevisiae*, purified it in soluble active form, and shown that it is necessary and sufficient to produce both asperlicin C and D in a constant ratio, indicating they derive from a common intermediate. These tetracyclic product regioisomers represent a dramatic morphing of the linear tripeptide backbone of Ant-Ant-Trp.

RESULTS

Expression and Purification of *A. alliaceus* AspA

To obtain the 276 kDa hexa-domain bimodular (A_1-T_1-C_2-A_2-T_2-C_T, where A is adenylation, T is thiolation, and C is condensation domains; C_T represents a terminal condensation domain at the end of the NRPS assembly line) NRPS AspA (Figure 1A) from *A. alliaceus* as a purified protein for catalytic characterization, we utilized *S. cerevisiae* strain BJ5464-NpgA that has vacuolar proteases deleted and contains a phosphopantetheinyl transferase (NpgA) that primes the apo forms of NRPS carrier domains (Ma et al., 2009). We previously found that this yeast strain will provide the TqaA trimodular NRPS in soluble, active form (Gao et al., 2012). The DNA encoding the *aspA* gene was cloned

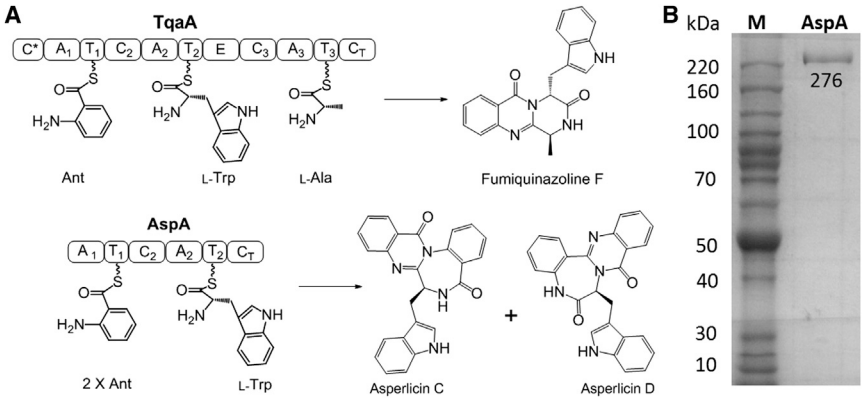

Figure 1. Heterologous Expression of AspA in *Saccharomyces cerevisiae*

(A) Amino acid building blocks for assembly of fumiquinazoline F (FQF) and asperlicins C and D. AspA is a 276 kDa two-module NRPS enzymes with the indicated adenylation (A), thiolation (T), and condensation (C) domains. The terminal condensation domains (C_T) of TqaA and AspA act as cyclization/release catalysts for Ant-d-Trp-L-Ala and Ant-Ant-L-Trp, respectively, presented as thioesters on the pantetheinyl arms of immediate upstream T domains. Intramolecular capture of the thioester carbonyl by the NH_2 of Ant_1 is the proposed common release mechanism. The subsequent transannular cyclizations and aromatizing dehydrations yield 6,6,6-tricyclic quinazolinedione (fumiquinazoline F) or tetracyclic 6,6,7,6 asperlicin C/D regioisomeric scaffolds, affected by the presence or absence of Ant_2 in the tripepitidyl-*S*-thiolation domain intermediates.

(B) SDS-PAGE gel of AspA expressed and purified from *S. cerevisiae* BJ5464-NgpA.

See also Table S1.

with RT-PCR; see Table S1 available online) in six sections and one intron of 63 base pairs (bp) was removed from fragment 1 before ligation to yield a 7,329 bp coding sequence, as described in the Experimental Procedures. The full-length *aspA* gene with a C-terminal His_6 tag was then moved into the *S. cerevisiae* strain for expression and affinity purification.

As shown in Figure 1B, the tagged AspA protein could be purified to apparent homogeneity in soluble form with a yield of 9 mg/l. No proteolytic fragments were detected, suggesting the six-domain protein is likely well folded.

Assay of the Adenylation Domains of AspA for Amino Acid Activation

The scaffolds of the suite of known asperlicin metabolites suggest that two molecules of Ant and one tryptophan are used as building blocks (Haynes et al., 2012). The purified AspA protein was assayed for the ability to form the aminoacyl-AMPs from Ant and L-Trp via amino acid-dependent exchange of radioactivity from $^{32}PP_i$ into ATP, a classical assay for reversible formation of acyl-adenylates (Linne and Marahiel, 2004). As shown in Figure 2A, Ant supports robust exchange activity with a k_{cat} = 1.6 s^{-1}, whereas L-Trp is also active with lower rates (k_{cat} = 1.5 min^{-1}, Figure S1). No significant activity was detected with other proteinogenic amino acids. Benzoate and salicylate as Ant analogs also gave evidence of reversible formation of the acyl-AMPs (Figure S1). Ant-L-Trp, Ant-D-Trp, and Ant-Ant dipeptides did not support exchange, suggesting they are not used as free intermediates (Figure 2A).

We also successfully cloned and expressed protein fragments spanning the two AspA modules. The A_1-T_1 construct was not solubly expressed but the A_1-T_1-C_2 tridomain (150 kDa) representing module 1 (M1) was soluble at a yield of 15 mg/l. Likewise A_2-T_2-C_T was not soluble, but the four-domain C_2-A_2-T_2-C_T (176 kDa) representing module 2 (M2) version was soluble at a yield of 10 mg/l (Figure S2). As shown in Figure 2A, these protein constructs allowed unambiguous assignment that the A_1 domain in M1 activates Ant; and A_2 in M2 activates L-Trp. This result therefore strongly indicates the iterative use of Ant by M1 in synthesis of the tripeptide. In addition, it was possible to express and purify in soluble form of the terminal C_T (52 kDa, yield 4 mg/l) and the didomain T_2-C_T (61 kDa, yield 16 mg/l) fragment from M2 (Figure S2), which proved useful in studies with di- and tripeptidyl-*S*-*N*-acetylcysteamine (SNAC) surrogate substrates noted later.

Holo-AspA Is Catalytically Competent to Generate Both Asperlicin C and D and Another Product Isomer

Having isolated the intact AspA protein and verified its A domains are catalytically active, we next examined if the bimodular NPRS can produce the tripeptidyl alkaloids. When 10 μM pure AspA was mixed with 1 mM Ant, 1 mM L-Trp, 3 mM ATP, and 5 mM $MgCl_2$ in 50 mM Tris-HCl at pH 7.5 for 16 hr and the small molecules analyzed with high-performance liquid chromatography (HPLC), Figure 3A shows major and minor peaks with the elution times of standard asperlicin C and asperlicin D (Haynes et al., 2012), respectively. Analysis of the peaks by mass spectrometry confirmed that both product peaks had m/z = 407 $[M + H]^+$, equal to that of both asperlicin C and D isomers (Figure S3). There is one additional enzyme-dependent minor product peak detectable in the HPLC traces, product **1**, and it too has the same m/z = 407 $[M + H]^+$ mass.

Rate assays under those conditions indicate linear formation rates for asperlicin C/D and the unknown product **1** (Figure 3B). Given the known extinction coefficients (almost the same at 280 nm) of the asperlicin C and D synthetic standards, the apparent turnover number for asperlicin C was calculated to be 126.1 ± 7.6 h^{-1} and that for asperlicin D is 12.0 ± 0.8 h^{-1}. That product ratio of ~10:1 does not change during the course of the incubation, suggesting the minor product asperlicin D is not forming from asperlicin C in a postreaction transformation, but is in fact an initially formed alternative product of AspA. Until the structure of the third isomeric product **1** is determined, we cannot confidently assign a turnover number to it. However, assuming that this asperlicin isomer might have a comparable A280 extinction coefficient, we would estimate an apparent turnover number of ~5.9 ± 0.3 h^{-1}, which represents 5% of the product flux that is also constant over the incubation time frame. Hence, all three products are likely

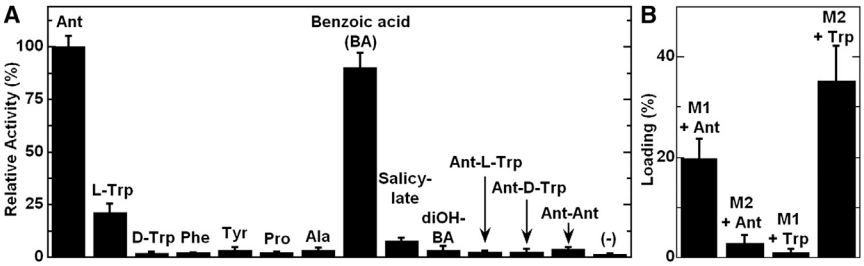

Figure 2. Anthranilate and l-Tryptophan Are Substrates of AspA

(A) ATP-[^{32}P]PP$_i$ exchange assay of full length AspA.

(B) Loading assay of A_1-T_1-C_2 (M1) and C_2-A_2-T_2-C_T (M2) with [^{14}C]anthranilate or [^{14}C]tryptophan. M1 activates Ant while M2 activates L-Trp. Assay components are labeled in the figure. Data represent mean values ± SD.

See also Figures S1 and S2.

derived from the same precursor, which we proposed to be an 11-membered macrolactam formed via macrocyclization of the tripeptide.

Assay of Truncated Forms of AspA for Product Formation: Activity of the Two Modules

To examine the iterative features of AspA, we dissected the AspA NRPS into M1 and M2. Mixing of the purified M1 and M2 with Ant, L-Trp, and ATP provided a reconstitution of asperlicin production with asperlicin C and D in the same ratio as full-length AspA and also the third minor product **1** (Figure S4). This validates that the dissected modules can work in *trans* and the tethered, activated anthranilyl moiety can be transferred productively to M2. It seemed likely that the second condensation domain C_2 would work twice in a catalytic cycle of AspA, first in the canonical mode to condense T_1-tethered Ant onto Trp-*S*-T_2 to yield Ant-L-Trp-*S*-T_2 and concomitantly free the thiol in T_1-*S*H (where -*S*-$T_\#$ designates the *S*-pantetheinyl thiolation domain in module #). If that Ant-L-Trp-*S*-enzyme had a sufficiently long lifetime, T_1 could reload with another Ant; a second round of transfer catalyzed by C_2 would generate Ant-Ant-L-Trp-*S*-T_2. We sought to test these two predictions by synthesis of dipeptidyl Ant-L-Trp-SNAC and tripeptidyl Ant-Ant-L-Trp-SNAC and adding them as surrogate substrates to particular purified fragments of AspA. The expectation was that HS-pantetheinyl-T_2 could engage in thioester exchange with the di- and tripeptidyl-SNACs to generate the corresponding Ant-L-Trp-*S*-T_2 and Ant-Ant-L-Trp-*S*-T_2 forms, respectively, to allow an evaluation of their catalytic competence.

To evaluate whether Ant-L-Trp-*S*-T_2 was on pathway, the purified terminal didomain T_2C_T (50 μM) was used and converted to the *holo* form by prior phosphopantetheinylation via the phosphopantetheinyltransferase Sfp and CoA-SH (Quadri et al., 1998). In parallel, *holo* M1 (50 μM) was incubated with Ant and ATP to produce the covalent Ant-*S*-T_1 form. Then the two proteins were combined, 400 μM synthetic Ant-L-Trp-SNAC was added, and product formation assayed after 1 hr. As shown in Figure 4A (trace ii), products with the diagnostic UV of asperlicins were detected; the anticipated pattern of asperlicin C/D and **1** were detected with liquid chromatography/mass spectroscopy (LC/MS) analysis with focus on extracted ion *m/z* = 407 [M + H]$^+$ (Figure S5). Nonenzymatic cyclization of Ant-L-Trp-SNAC to the bicyclic benzodiazepinedione and hydrolysis of the thioester to Ant-L-Trp acid compete with the enzymatic consumption as we have reported previously (Gao et al., 2012). In the absence of the AspA fragments, these spontaneous products were detected (Figure 4A, trace i). Figure 4B shows the proposed acyl exchange between SNAC and HS-pantetheinyl-T_2 to yield the Ant-L-Trp-*S*-T_2, which is competent to receive the Ant moiety on T_1 and proceed through the catalytic cycle.

T_2C_T Bidomain Converts Ant-Ant-L-Trp-SNAC to the Suite of Asperlicin Products

These results suggest that Ant-Ant-L-Trp-*S*-T_2 will be formed from Ant-*S*-T_1 and Ant-L-Trp-*S*-T_2 during the AspA catalytic cycle (Figure 4B). To evaluate that directly we prepared the corresponding Ant-Ant-L-Trp-SNAC and added it to either the purified C_T domain or to the purified T_2C_T protein construct. As shown in Figure 5A (trace iv), no asperlicins are generated in the absence of AspA fragments, demonstrating the tripeptidyl thioester (unlike the Ant-Trp-SNAC) is stable in solution and any cyclization requires the action of an enzyme, most likely the C_T. However, the isolated C_T domain was incompetent (trace iii) but the T_2C_T (trace i) generated the characteristic trio of asperlicin products at *m/z* = 407 [M + H]$^+$ in the presence of the tripeptide-SNAC as assessed in an overnight incubation (Figure S6). Thus, the T_2 domain appears essential in recognition/presentation of the tripeptide by the C_T domain. In a previous study of ours (Gao et al., 2012), the same requirement held for presentation of Ant-d-Trp-L-Ala to the C_T domain of TqaA as a thioester bound to the immediately upstream T in that fumiquinazoline F-generating trimodular NRPS. In the absence of CoA and Sfp, an assay containing T_2C_T still produced ~80% yield of the same product mixture as shown in trace ii. Taken together, we propose asperlicin formation in traces i and ii was initiated by the nonenzymatic transfer of the Ant-Ant-L-Trp moiety from SNAC to the HS-pantetheinyl arm of T_2 (Figure 5B) through thioester interchange. At that juncture, the downstream C_T domain can catalyze the intramolecular amide bond formation(s) that constitutes release of the nascent cyclic product.

Proposed Cyclization Mechanisms of Asperlicin C and D and Computation Prediction of Product Distributions

Insight into that common released precursor from AspA comes from inspection of the differences between the isomeric asperlicin C and D and their molecular connectivity (Figure 6). The mechanistic assumption, which is supported by the reconstitution studies with intact and dissected AspA, is that the linear Ant-Ant-Trp-*S*-T_2, tripeptidyl-*S*-enzyme is a late intermediate. The terminal condensation domain C_T would then act to release the tripeptidyl chain by cyclization, analogous to that demonstrated role by the C_T domain of TqaA as it releases tricyclic fumiquinazoline F (Gao et al., 2012). While an alternative macrocyclization mechanism may be considered as detailed in the Discussion, the aniline NH_2 of Ant_1 will likely be the most competent nucleophile (Figure 6A). That release step (attack of N_8 on

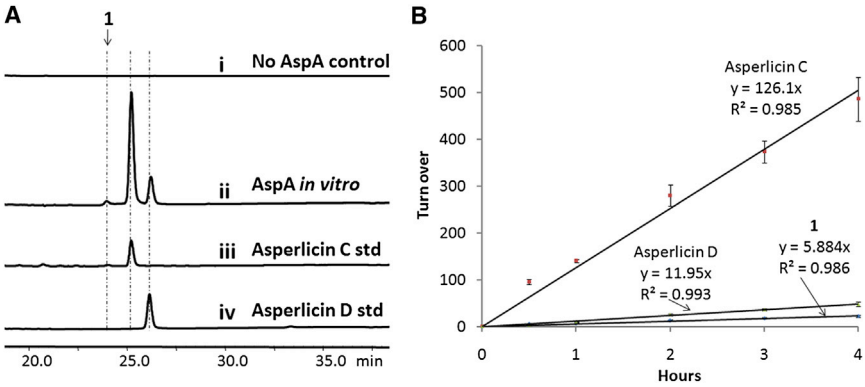

Figure 3. In Vitro Reconstitution of AspA
(A) LC/MS analysis (280 nm) shows purified AspA generates asperlicin C/D and a third product **1** of identical mass from Ant, L-Trp, and ATP;
(B) Catalytic turnover number and product partition ratios for **1**, asperlicin C and D production. Both asperlicin C and D standards were synthesized from our previous study (Haynes et al., 2012). Data represent mean ± SD. Also see Figures S3 and S4.

[C_7 = O]) would generate a tricyclic product 6,11,6-macrocycle **I**, fully analogous to the 6,10-bicyclic product (vide infra) we have proposed in TqaA action to generate fumiquinazoline F (FQF) (Gao et al., 2012; Figure 1). As shown in Figure 6A, the 11-membered macrocycle **I** could be subject to transannular attack with three different regiochemistries, by attack of each of the three amide nitrogen (N_1, N_5, N_8) on one of the three carbonyls ([C_4 = O], [C_7 = O], or [C_{11} = O]).

Attack of N_1 on (C_7 = O) across the ring generates a six-membered and a seven-membered ring, converting the nascent macrocycle **I** into a tetracyclic framework. Loss of water from the initial addition product yields the major product (~85% of the final product flux) asperlicin C. Alternatively, amide N_5 could capture (C_{11} = O). This also builds additional six- and seven-membered rings, generating a regioisomeric tetracyclic scaffold, a dehydration step away from the minor product asperlicin D (~10% of the flux). A third potential route would be transannular attack of N_8 on (C_4 = O). That would generate a third regiosiomer, at the same mass of 406, but now with an angular 6,8,6,5 tetracyclic scaffold. The very minor product **1** with the identical mass could be this third isomer, but we were not able to isolate it in sufficient quantity to prove structure.

To gain insight into the energetics of the three different modes of cyclization, we performed quantum mechanical calculations on the free energy changes (ΔΔG) associated with each of the products shown in Figure 6 (See Computational Details in the Experimental Procedures). Interestingly, and as shown in Figure 7, asperlicin D is the most stable product among the three, while the structure proposed for product **1** in Figures 6 and 7 is much higher in energy. However, examination of other possible cyclization outcomes of macrocycle **I** suggests that this is the most likely option. These results suggest that not the thermodynamic stability of the three possible adducts, but kinetic factors determine the regiochemical outcome of the reaction. As also shown in Figure 7, starting from the 6,11,6-macrocycle **I**, different *trans* to *cis* isomerizations of the peptide bonds must take place to reach conformations suitable for cyclization. These are shown as macrocycles **II**, **III**, and **IV** in Figure 7 and are appropriate for formation of asperlicin C, D, and **1**, respectively. The idea here is similar to Bruice's NAC, or "near-attack conformation" (Bruice, 2002; Bruice and Lightstone, 1999; Hur and Bruice, 2003). Macrocycle **II**, the corresponding transition state (**TS2**) leading to asperlicin C entails the most favorable pathway, while the precursors to asperlicin D are much higher in energy, consistent with the observed 10:1 ratios of asperlicin C/D (Figure 7). In view of these results, it can be hypothesized that C_T domain is responsible for recognizing and stabilizing the adequate conformation of the 6,11,6-macrocycle by promoting the isomerization of the N_5–C_4 = O peptide bond and directing the formation of asperlicin C. To what extent such nascent products are released and cyclized nonenzymatically or are cyclodehydrated on the way out of the active site of the C_T domain of AspA is a subject for subsequent evaluation.

We note that an alternate route of intramolecular release of an Ant-Ant-L-Trp-*S*-T_2 could be imagined, via formation of an anthranilyl-diketopiperazine. This would involve amide N_5 attack (from the Ant_2 residue) on the tripeptidyl thioester carbonyl (C_{11} = O) as the chain release step (Figure 6B). Whether that amide would be a kinetically competent nucleophile compared to the Ant_1 free NH_2 groups seems less likely. Moreover, while that putative diketopiperazine (DKP) could then undergo cyclization and dehydration to asperlicin C, it has the wrong connectivity to get to the observed asperlicin D framework, as noted in Figure 6B. Thus, the DKP release route is ruled out and formation of the 6,11,6-tricyclic macrocycle **I** seems the likely mechanism of AspA.

DISCUSSION

Our initial identification of the *aspABC* gene cluster(Haynes et al., 2012) by sequencing of the *A. alliaceus* genome relied on gene knockouts of *aspA* and *aspB*, the NRPS- and epoxygenase-encoding genes respectively, and the accumulation of different asperlicins in extracts from those mutants. We had synthesized authentic samples of asperlicin C and asperlicin D both as standards and to evaluate their capacity to serve as substrates for purified AspB, the indole epoxygenase (Haynes et al., 2012). Given that pure AspB acted selectively on asperlicin C (to yield asperlicin E) and not asperlicin D, we concluded that while asperlicin D was a natural *Aspergillus* metabolite (Liesch et al., 1988), it was a dead end for subsequent processing to either asperlicin E or asperlicin itself. The question remained how and why asperlicin D formed as a coproduct with asperlicin C.

In this study, we have turned to characterization of the NRPS AspA enzyme. Bioinformatic analysis of AspA from the genome sequence predicted it would have only two modules (A_1-T_1-C_2-A_2-T_2-C_T) (Haynes et al., 2012), whereas asperlicin C and D are comprised of three amino acid units, two molecules of Ant, and one Trp. Thus, a question at the start of this study was whether there was an additional, missing, monomodular NRPS

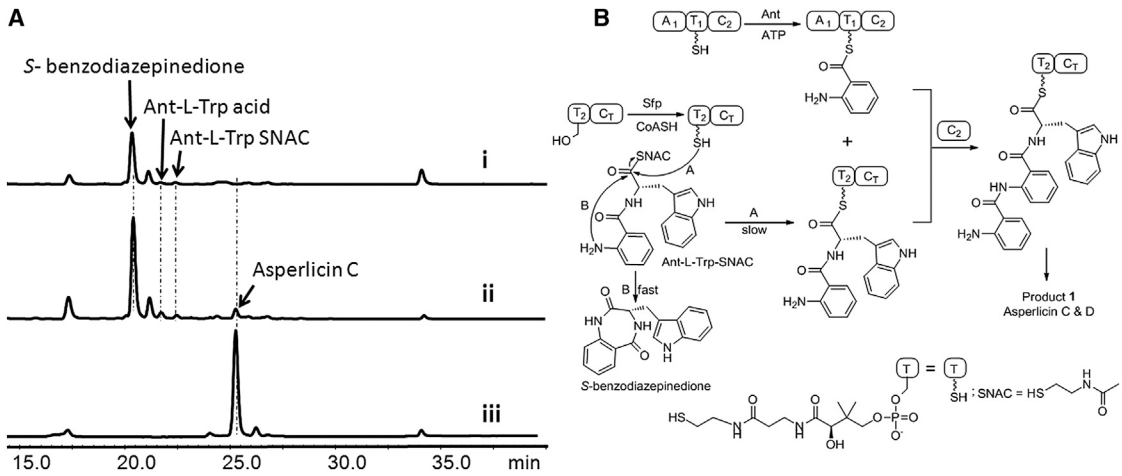

Figure 4. The First Module of AspA Iteratively Uses Two Molecules of Ant

(A) The dipeptidyl Ant-L-Trp-SNAC (Gao et al., 2012) is a surrogate substrate for M2 of AspA: the *holo* form of M1 (50 μM A_1-T_1-C_2) was preloaded with Ant (1 mM Ant, 3 mM ATP) for 1 hr while in parallel the T_2-C_T didomain was converted to the *holo* (HS-pantetheinyl) form using 20 μM Sfp and 1 mM CoASH. The two solutions were mixed with addition of 400 μM Ant-L-Trp-SNAC and incubated overnight before aliquots were analyzed by LC/MS (280 nm). Trace i shows the spontaneous products (*S*-benzodiazepinedione and Ant-L-Trp acid) formed from an assay without T_2C_T didomain; trace ii shows products formed from an assay including *holo* T_2C_T. In addition to the spontaneously formed products, formation of asperlicin C can be detected. Trace iii shows the profile of products formed from full length AspA starting from Ant, L-Trp and ATP.

(B) Reaction scheme: M1 loaded covalently with Ant on the pantetheinyl arm of T_1 reacts with Ant-L-Trp-*S*-pantetheinyl-T_2-C_T to yield the tripeptidyl Ant-Ant-L-Trp-*S*-T_2-C_T form of the bi-domain T_2-C_T protein fragment. That can be acted on by C_T to yield asperlicin C, D and **1**. The added Ant-L-Trp-SNAC is proposed to undergo acyl exchange onto the HS-pantetheinyl arm of T_2-C_T in competition with hydrolysis to Ant-L-Trp and intramolecular cyclization to *S*-benzodiazepinedione.

See also Figures S5 and S7.

to produce a third module, on which a tripeptidyl (Ant-Ant-L-Trp)-thioester could be tethered. Alternatively, it was possible that bimodular AspA could act twice on Ant and generate a linear tripeptidyl-*S*-T_2 intermediate to be released by cyclizing action of the C_T domain (Gao et al., 2012).

To address whether AspA is sufficient to generate and release both asperlicin C and asperlicin D, we constructed a C-terminal His_6-tagged version of the 276 kDa AspA for expression in the vacuole protease-deficient *S. cerevisiae* strain BJ5464-NpgA. This strain has been of use to us for cloning the comparably sized bimodular AnaPS as well as the trimodular TqaA in aszonalenin and tryptoquialanine pathways, respectively (Gao et al., 2012). Soluble AspA with the pantetheinyl-SH prosthetic groups installed posttranslationally on T_1 and T_2 was thereby obtained in a yield approaching 9 mg/l, suitable for biochemical characterization.

First, we assayed the capacity of *holo* AspA to activate Ant and L-Trp by reversible formation of the aminoacyl-AMPs and validated that each A domain was active. Because both A_1 and A_2 are contained in the same protein, one could not determine from such radioactive exchange assays if A_1 was activating Ant and A_2 was activating Trp, or A_2 activated both Ant and Trp. To that end, the expression and separate purification of C-terminally His_6-tagged M1 (A_1-T_1-C_2) and M2(C_2-A_2-T_2-C_T) allowed that distinction. Inclusion of C_2 in both constructs was necessary to achieve soluble expression of A domain-containing fragments. The A_1-containing protein activated Ant and the A_2-containing module activated L-Trp as Trp-AMP but did not act on Ant. The two-module AspA assembly line thus tethers Ant to T_1 and L-Trp to T_2. The Ant-Ant and Ant-Trp dipeptides were not substrates for either A_1 or A_2 (Figure 2A). If A_1 made an Ant-Ant-tethered thioester before transferring to Trp-*S*-T_2, one might have expected detection of the cyclic Ant-Ant dimer. No such dimer was detected from A_1-T_1-C_2 incubations with Ant and ATP (Figure S7). Mixing the M1 and M2 reconstituted asperlicin C and D formation as efficiently as the intact AspA, proving the separate modules could function in *trans*, and that the second copy of the C_2 domain was not a problem for reconstitution (Figure S4). M1 acts iteratively, first to generate a canonical Ant-Trp-*S*-T_2 that is then elongated by a reloaded Ant-*S*-T_1 to provide the Ant-Ant-Trp-*S*-T_2 as a full-length intermediate that undergoes release by intramolecular cyclization.

Full length, purified AspA is clearly sufficient to make the tetracyclic scaffold of asperlicin C from 2 molecules of Ant, 1 L-Trp. It also generates asperlicin D, a known *A. alliaceus* minor metabolite. In this study, a 10:1 constant ratio of asperlicin C:D is observed by kinetic analysis because asperlicin D represents ~10% of the product flux. The constant ratio indicates that both products are formed from a common intermediate or nascent product. From the failure of asperlicin D to be carried forward by AspB, the epoxygenation enzyme that takes asperlicin C on to asperlicin E (Haynes et al., 2012), we have reasoned that asperlicin D is a dead-end metabolite and so represents off-pathway partitioning of a common precursor. The mixture of asperlicin C and D (and **1**) are also produced in the two-module reconstitution experiment as well as in the incubations with Ant-Trp-SNAC and Ant-Ant-Trp-SNAC as surrogate substrates to probe the nature of later stage intermediates during AspA catalysis. Computational analysis clearly indicated that while asperlicin D is more stable, asperlicin C is the kinetically

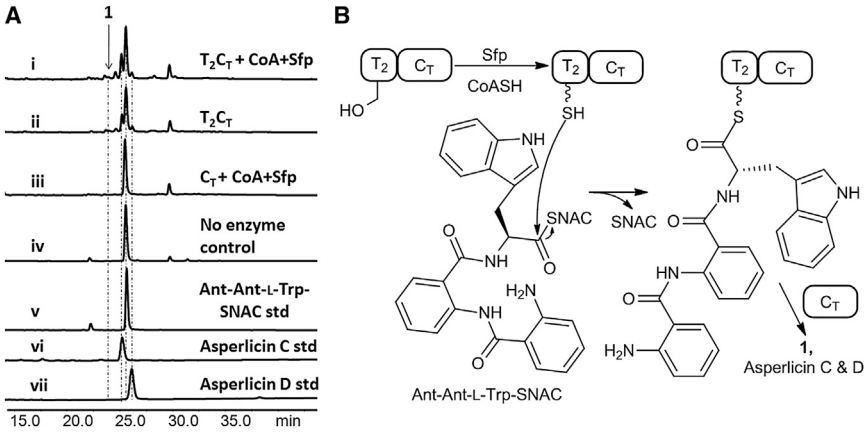

Figure 5. The T_2C_T Didomain Fragment of AspA Generates Asperlicin C and D from Exogenous Ant-Ant-l-Trp-SNAC

(A) UV-vis analyses of HPLC traces (280 nm) from the indicated incubations are shown. Reactions contained 50 mM Tris-HCl buffer, pH 7.5, in 100 μl. Reactions represented by traces i to iv contained 100 μM Ant-Ant-L-Trp-SNAC. Fifty micromolar T_2C_T, 20 μM Sfp, and 2 mM CoASH were added to reaction I; but only 50 μM T_2C_T was added in reaction ii; 50 μM C_T, 20 μM Sfp, and 2 mM CoASH were added in reaction iii; No enzyme was added in reaction iv. Traces (v–vii) are standards. The suite of asperlicin C, D, and **1**($[M+H]^+$ = 407) are found in traces i and ii but not in iii and iv.

(B) Reaction scheme featuring nonenzymatic acyl exchange from the -SNAC to the T_2 domain pantetheinyl thiol arm to yield the tripeptidyl-*S*-T_2 covalent enzyme as substrate for cyclizing release by the downstream C_T domain.

See also Figures S6 and S7.

favored product, thereby explaining the observed preference in the formation of asperlicin C from AspA. The extent to which C_T domain influences the near attack conformation of the macrolactam in its active site is unclear. However, it is evident that the formation of asperlicin D cannot be suppressed under experimental conditions (both in vivo and in vitro), thereby giving support to a mechanism of transannular cyclization in which the outcomes are dictated by free-energy barriers.

The AspA NRPS illustrates the unusual cyclopeptide ring sizes attainable in the asperlicin system and is distinct from the related fumiquinazoline and ardeemin systems, where comparable 6,10-bicyclic nascent products gave rise to regioisomeric tricyclic quinazolinedione scaffolds (Gao et al., 2012; Figure 1). In both cases we argue that the terminal C_T domains are the chain release catalysts by intramolecular capture of the thioester carbonyl by the Ant_1-NH_2 group, yielding a 6, 10 (TqaA) or 6,11,6 (AspA) tricyclic nascent product. Subsequent closure to the very different 6,6,6-tricyclic versus 6,6,7,6-tetracyclic scaffold reflects the use of an additional Ant unit in the second position of the tripeptide framework, uniquely in the asperlicin assembly line. One planar β-amino acid unit (Ant) at the amino terminus of a tripeptidyl thioester directs cyclization to the tricyclic quinazolinedione framework. The second Ant β-aminoacyl building block adds another carbon and incorporates the fourth ring into the final asperlicin scaffolds.

While we proposed that the aniline amine on the first Ant residue is responsible for initiating the macrolactam formation, there are alternative nucleophiles that may be considered to initiate the cascade of reactions. As shown in Figure S8, in addition to the possibility that the aniline nitrogen serves as the product-releasing nucleophile (mechanism 3), two alternative mechanisms can be envisioned. In mechanism 1, the (C_4 = O) carbonyl oxygen in imide form could be sufficiently nucleophilic to first attack the thioester to generate an oxazol-5(4H)-one ring, followed by attack of the (C_{11} = O) carbonyl oxygen and undergo ring expansion to yield a nine-membered ring, which can then be opened to the 6,11,6-macrocylce **I**. Alternatively in mechanism 2, the amide nitrogen bridging the two Ant residues can initiate attack on the thioester to form a seven-membered ring, followed by ring expansion to the 6,11,6-macrocycle **I**.

To assess the possibilities of these routes, we computed the relative free energies of each transition state and product among the three possible mechanisms (see Computational Details in the Experimental Procedures). To locate and characterize transition structures for these reactions, fully deprotonated nucleophiles (both amides and anilines) were used despite the low acidities of the aniline and amide groups (Figure S9) to locate neutral TS including explicit solvation and a general base. Such reactions require general base catalysis, and this is assumed to take place in the enzyme active site. The inclusion of a general base and solvent would be necessary to compute the barriers to various reactions occurring in water or the enzyme. Our calculations therefore only test the factors aside from deprotonation energetics that are required to distort the different intermediates along the reaction coordinate into various transition state geometries. The energetics of deprotonation of different nucleophiles by bases would be contributors to the actual free energies of reaction. As shown in Figure S8, while formation of the oxazolone product in mechanism 1 is kinetically possible ($\Delta\Delta G^{\ddagger}$ = 14 kcal/mol), it represents a thermodynamic dead-end that is unlikely to undergo additional modifications. In fact, subsequent ring expansion reactions toward either nine-membered or seven-membered rings are kinetically unfeasible ($\Delta\Delta G^{\ddagger}$ > 35 kcal/mol). In mechanism 2, calculations showed that the attack of the amidate nitrogen to form the seven-membered ring is highly unfavorable ($\Delta\Delta G^{\ddagger}$ = 34 kcal/mol) and is therefore unlikely to take place. In contrast, the direct attack of the aniline in mechanism 3 is the favored pathway because the activation barrier is low ($\Delta\Delta G^{\ddagger}$ = 13 kcal mol^{-1}). These results are in good agreement with the observed nonenzymatic reactivity of dipeptide Ant-l-Trp-SNAC, which undergoes fast cyclization exclusively through the terminal aniline.

In conclusion, we have focused on the mechanism of AspA-catalyzed formation of asperlicin C and D. In a previous study we showed that the monooxygenase AspB will take asperlicin C and perform an oxygenative cyclization to produce asperlicin E, now with a fused heptacyclic framework (Haynes et al.,

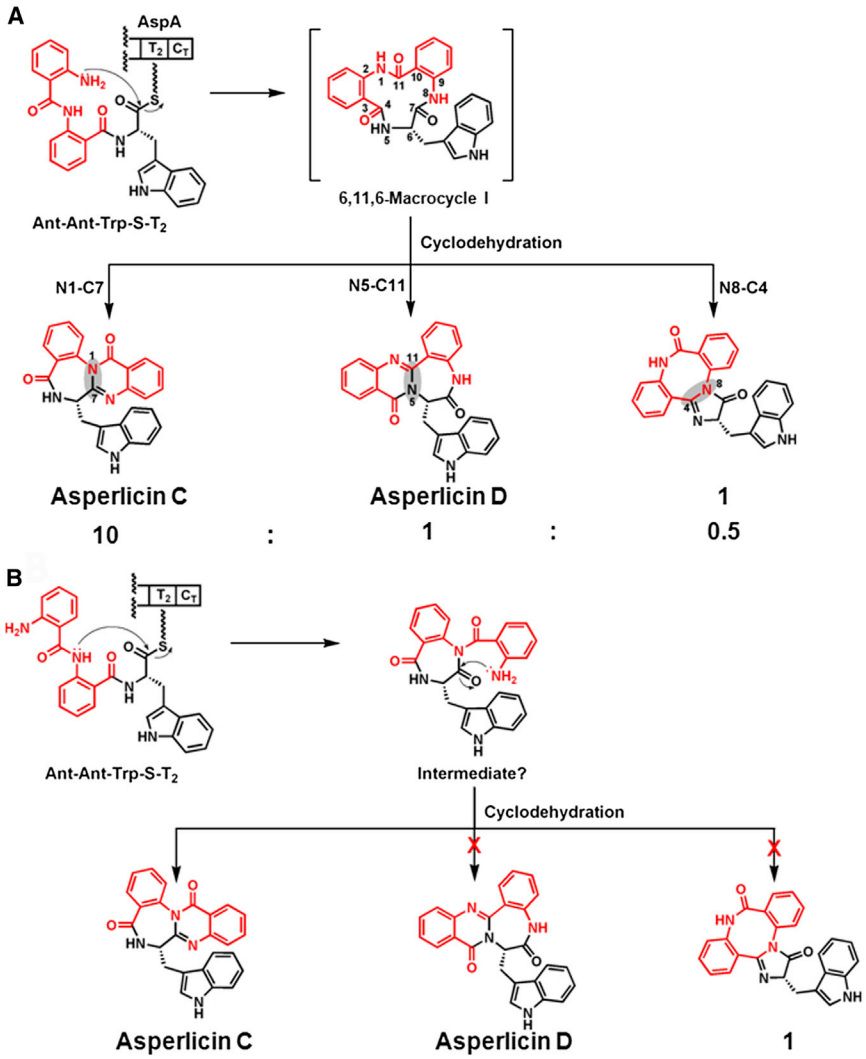

Figure 6. Mechanistic Proposal for Generation of a Constant Ratio of Asperlicin C and Asperlicin D from Macrocyclizing Release of a Linear Ant-Ant-L-Trp-S-T_2 Thioester by the C_T Domain

(A) The attack of the free NH_2 of the Ant_1 residue generates a transient 6,11,6-tricyclic product macrocycle (**I**). Subsequent transannular attack and dehydration can proceed with distinct regiochemistries of intramolecular amide capture of carbonyl groups: N_1 on $C_7 = O$ gives major product asperlicin C, N_5 on $C_{11} = O$ gives asperlicin D, while N_8 on $C_4 = O$ could give a third asperlicin regioisomer, putative product **1**. Whether these steps happen in one of the active sites of AspA or in solution have not yet been determined.

(B) Alternative mode of tripeptidyl chain release by initial attack of the amide NH of Ant_2 residue on the thioester carbonyl would yield a diketopiperazine as nascent product. That can go on to asperlicin C as shown but has the wrong connectivity to generate the observed minor product asperlicin D and **1** and so is ruled out.

2012). This is a remarkable complexity generation from a two-enzyme pathway with economical strategy and catalytic execution.

SIGNIFICANCE

Fungal peptidyl alkaloids represent a group of compounds with diverse chemical structures and important biologic activities. The planar nonproteinogenic amino acid, anthranilate (Ant), is an important building block in many bioactive fungal peptidyl alkaloids. Here, we heterologously expressed the bimodular NRPS AspA in *Saccharomyces cerevisiae* and successfully reconstituted AspA to produce the regioisomers asperlicin C and D in vitro. Significantly, differing from the canonical, colinear programming rule of NRPSs, in which every module activates and appends one amino acid to the growing peptide, we showed the first module of AspA iteratively uses two molecules of Ant to build the Ant-Ant-Trp tripeptide precursor. The C-terminal condensation domain (C_T) was demonstrated to cyclize the linear tripeptide and to produce a macrocycle that can undergo different intramolecular cyclization fates. Experimental and computational studies were performed to examine the regioselectivity and energetics of this step, which showed the kinetically most favored product asperlicin C dominates over the thermodynamically more stable product asperlicin D.

EXPERIMENTAL PROCEDURES

Cloning of Intact *aspA* Gene from *A. alliaceus*

The AspA encoding gene was assembled from six pieces (P1–P6, each ~1–1.5 kb) by using modified yeast-based homologous recombination methods (Gao et al., 2012; Table S1). The only intron (493–555 base pairs [bp]) in the *aspA* gene was found with RT-PCR and no other introns were found in other regions. The assembled AspA expression plasmid was recovered from *S. cerevisiae* using a yeast plasmid miniprep II kit (Zymo Research) and was verified by restriction digestion and PCR. Protein expression and purification procedures are described in the Supplemental Experimental Procedures.

ATP-[^{32}P]PP_i Exchange Assay for AspA

A typical reaction mixture (500 μl) contained 1.0 μM AspA, 1 mM substrate (unless specified), 5 mM ATP, 10 mM $MgCl_2$, 5 mM Na[^{32}P]pyrophosphate (PP_i) (~1.8 × 10^6 cpm/ml), and 100 mM Tris-HCl (pH 8). Mixtures were incubated at ambient temperature for regular time intervals (e.g., 5 min), and 150 μl aliquots were removed and quenched with 500 μl of a charcoal suspension (100 mM NaPPi, 350 mM $HClO_4$, and 16 g/l charcoal). The mixtures were vortexed and centrifuged at 13,000 rpm for 3 min. Pellets were washed twice with 500 μl of wash solution (100 mM NaPPi and 350 mM $HClO_4$). Each pellet was resuspended in 500 μl wash solution and added to 10 ml Ultima Gold scintillation fluid. Charcoal-bound radioactivity was measured using a Beckman LS 6500 scintillation counter.

Loading of ^{14}C-Substrate onto NRPS

A 50 μl assay mixture containing 100 mM HEPES (pH 7), 10 mM $MgCl_2$, 2 mM ATP, 1mM TCEP, 10 μM AspA-M1/M2, and 40 μM ^{14}C-labeled substrate

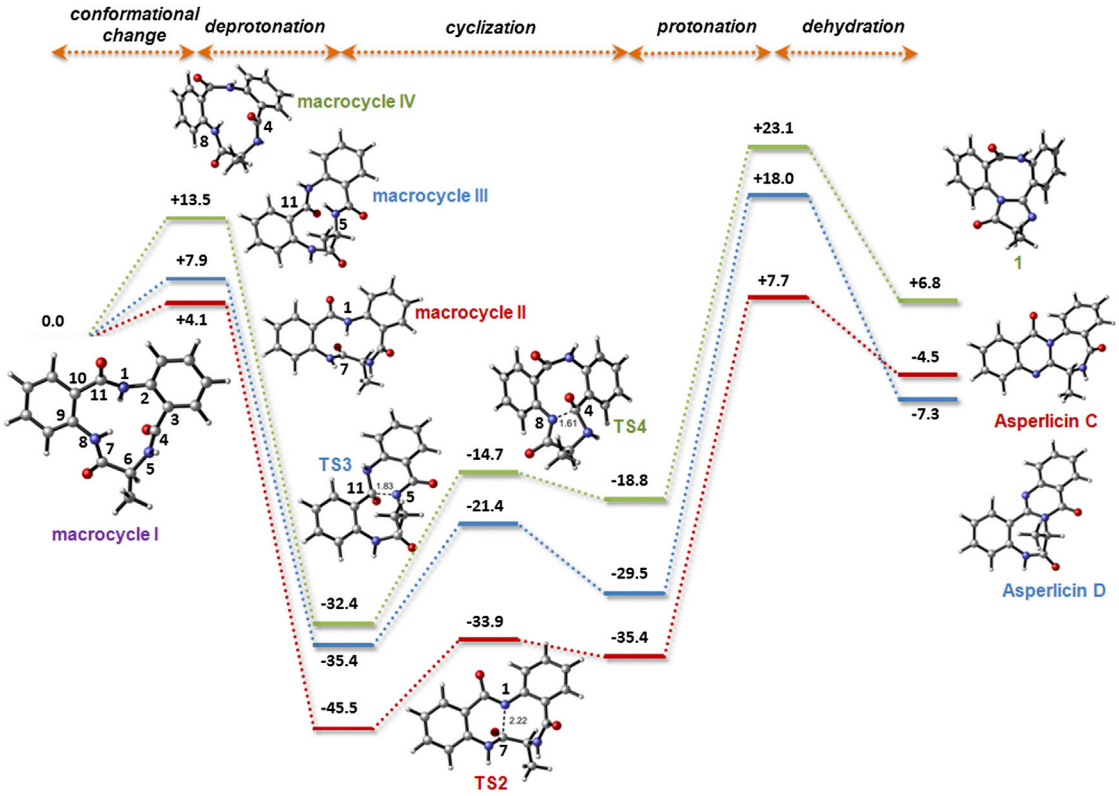

Figure 7. Structures and Relative Energies Calculated for the Different Conformations of the Initial Macrocycle, Cyclization Transition States, and Final Dehydrated Products Relevant to the Biosynthesis of Asperlicin C, D, and 1

The calculations were performed at the PCM(water)/B3LYP/6-31G(d) level using reduced models in which the indole ring from Trp side chain has been replaced by a methyl group. Amide bonds subjected to isomerization from *trans* to *cis* orientation prior to cyclization are marked in blue. Relative free energies are in kcal/mol and distances in angstroms.

See also Figures S8 and S9.

(anthranilate or tryptophan) was incubated at ambient temperature for 30 min. The reaction was quenched by 600 μl 10% trichloroacetic acid with the addition of 100 μl of 1 mg/ml BSA. The mixture was vortexed and centrifuged at 13,000 rpm for 3 min. The pellet was then washed twice with 600 μl 10% trichloroacetic acid, dissolved in 250 μl formic acid, added into 10 ml Ultima Gold scintillation fluid, and subjected to a Beckman LS 6500 scintillation counter.

Synthesis of Ant-Ant-L-Trp-SNAC

Tripeptide Ant-Ant-L-Trp was custom synthesized by GenScript USA (Piscataway, NJ). Thirty milligrams Ant-Ant-L-Trp (1.0 eq), 140 mg PyBOP (4.0 eq), 37 mg K_2CO_3 (4.0 eq), and 145 μl *N*-acetylcysteamine (SNAC) (20 eq) were dissolved in 20 ml H_2O:THF (1:1). The solution was stirred at room temperature for 2 hours. The mixture was concentrated in vacuo, dissolved in acetonitrile, and purified by prep-HPLC (Luna, C18 250 × 21.2 mm, 10 μm, 100 Å) using a chromatographic gradient: 20%–40% B, 5 min; 40%–80% B, 25 min; 80%–100% B, 5 min (A: H_2O; B: acetonitrile, 10 ml/min, monitor at 340 nm). The peak with expected mass (*m/z* calculated for Ant-Ant-Trp-SNAC $C_{29}H_{29}N_5O_4S$ $[M+H]^+$ 544.2013, found 544.2023) was collected and lyophilized. The final yield is 19.6 mg (53%).

HPLC-Based Time Course Study of Product Formation by AspA

Master reactions (500 μL) contained 1 μM AspA, 3 mM ATP, 2 mM $MgCl_2$, and 1 mM amino acid substrates (Ant and l-Trp) and AspA in 50 mM Tris-HCl buffer (pH 7.5) were carried out at 25°C and 100 μl aliquots at 1, 2, 3, and 4 hr time points were quenched by adding 1 ml of ethyl acetate. The initial product turnover rates were calculated with mean values ± SD by using the data points within the linear range. The ethyl acetate layer was dried and redissolved in methanol (100 μl), and 20 μl samples were subjected to LC/MS analyses. Peak areas (at 280 nm) of the asperlicin C, aperlicin D, and **1** were converted to concentrations and were used to calculate the initial enzymatic rate (μM/hr).

Computational Details

Calculations were carried out with the B3LYP hybrid functional (Becke, 1993; Lee et al., 1988) and 6-31G(d) basis set. Full geometry optimizations and transition structure (TS) searches were carried out with the Gaussian 09 package (Gaussian, Wallingford, CT). The possibility of different conformations was taken into account for all structures, and only the lowest energy structures are discussed. Frequency analyses were carried out at the same level used in the geometry optimizations, and the nature of the stationary points was determined in each case according to the appropriate number of negative eigenvalues of the Hessian matrix. The harmonic oscillator approximation in the calculation of vibration frequencies was replaced by the quasiharmonic approximation developed by Cramer and Truhlar (Ribeiro et al., 2011). Scaled frequencies were not considered since significant errors in the calculated thermodynamic properties are not found at this theoretical level (Bauschlicher, 1995; Merrick et al., 2007). Where necessary, mass-weighted intrinsic reaction coordinate (IRC) calculations were carried out by using the Gonzalez and Schlegel scheme (Gonzalez and Schlegel, 1989, 1990) to ensure that the TSs indeed connected the appropriate reactants and products. Bulk solvent effects were considered implicitly by performing single-point energy calculations on the gas-phase optimized geometries, through the SMD polarizable continuum model of Cramer and Thrular (Marenich et al., 2009) as implemented in Gaussian 09. The internally stored parameters for water were used to calculate solvation free energies (ΔG_{solv}).

SUPPLEMENTAL INFORMATION

Supplemental Information includes Supplemental Experimental Procedures, nine figures, and one table and can be found with this article online at http://dx.doi.org/10.1016/j.chembiol.2013.04.019.

ACKNOWLEDGMENTS

Dr. Timothy A. Wencewicz is thanked for analyses of the macrocyclizing mechanism and helpful discussions in synthesizing the Ant-Ant-L-Trp-SNAC substrate. Dr. Stuart W. Haynes is thanked for providing the Ant-L-Trp-SNAC substrate and asperlicin C/D standards. We thank the National Institutes of Health for funding (GM020011 and GM049338 to C.T.W., GM092217 to Y.T., and GM075962 to K.N.H.).

Received: March 5, 2013
Revised: April 24, 2013
Accepted: April 30, 2013
Published: July 25, 2013

REFERENCES

Ames, B.D., and Walsh, C.T. (2010). Anthranilate-activating modules from fungal nonribosomal peptide assembly lines. Biochemistry *49*, 3351–3365.

Ames, B.D., Liu, X., and Walsh, C.T. (2010). Enzymatic processing of fumiquinazoline F: a tandem oxidative-acylation strategy for the generation of multicyclic scaffolds in fungal indole alkaloid biosynthesis. Biochemistry *49*, 8564–8576.

Ames, B.D., Haynes, S.W., Gao, X., Evans, B.S., Kelleher, N.L., Tang, Y., and Walsh, C.T. (2011). Complexity generation in fungal peptidyl alkaloid biosynthesis: oxidation of fumiquinazoline A to the heptacyclic hemiaminal fumiquinazoline C by the flavoenzyme Af12070 from *Aspergillus fumigatus*. Biochemistry *50*, 8756–8769.

Bauschlicher, C.W., Jr. (1995). A comparison of the accuracy of different functionals. Chem. Phys. Lett. *246*, 40–44.

Becke, A.D. (1993). Density-functional thermochemistry. III. The role of exact exchange. J. Chem. Phys. *98*, 5648–5652.

Bok, J.W., Hoffmeister, D., Maggio-Hall, L.A., Murillo, R., Glasner, J.D., and Keller, N.P. (2006). Genomic mining for *Aspergillus* natural products. Chem. Biol. *13*, 31–37.

Bruice, T.C. (2002). A view at the millennium: the efficiency of enzymatic catalysis. Acc. Chem. Res. *35*, 139–148.

Bruice, T.C., and Lightstone, F.C. (1999). Ground state and transition state contributions to the rate of intramolecular and enzymic reactions. Acc. Chem. Res. *32*, 127–136.

Chang, R.S.L., Lotti, V.J., Monaghan, R.L., Birnbaum, J., Stapley, E.O., Goetz, M.A., Albers-Schönberg, G., Patchett, A.A., Liesch, J.M., Hensens, O.D., et al. (1985). A potent nonpeptide cholecystokinin antagonist selective for peripheral tissues isolated from *Aspergillus alliaceus*. Science *230*, 177–179.

Finking, R., and Marahiel, M.A. (2004). Biosynthesis of nonribosomal peptides1. Annu. Rev. Microbiol. *58*, 453–488.

Gao, X., Chooi, Y.-H., Ames, B.D., Wang, P., Walsh, C.T., and Tang, Y. (2011). Fungal indole alkaloid biosynthesis: genetic and biochemical investigation of the tryptoquialanine pathway in *Penicillium aethiopicum*. J. Am. Chem. Soc. *133*, 2729–2741.

Gao, X., Haynes, S.W., Ames, B.D., Wang, P., Vien, L.P., Walsh, C.T., and Tang, Y. (2012). Cyclization of fungal nonribosomal peptides by a terminal condensation-like domain. Nat. Chem. Biol. *8*, 823–830.

Gonzalez, C., and Schlegel, H.B. (1989). An improved algorithm for reaction path following. J. Chem. Phys. *90*, 2154–2161.

Gonzalez, C., and Schlegel, H.B. (1990). Reaction path following in mass-weighted internal coordinates. J. Chem. Phys. *94*, 5523–5527.

Haynes, S.W., Ames, B.D., Gao, X., Tang, Y., and Walsh, C.T. (2011). Unraveling terminal C-domain-mediated condensation in fungal biosynthesis of imidazoindolone metabolites. Biochemistry *50*, 5668–5679.

Haynes, S.W., Gao, X., Tang, Y., and Walsh, C.T. (2012). Assembly of asperlicin peptidyl alkaloids from anthranilate and tryptophan: a two-enzyme pathway generates heptacyclic scaffold complexity in asperlicin E. J. Am. Chem. Soc. *134*, 17444–17447.

Haynes, S.W., Gao, X., Tang, Y., and Walsh, C.T. (2013). Complexity generation in fungal peptidyl alkaloid biosynthesis: a two-enzyme pathway to the hexacyclic mdr export pump inhibitor ardeemin. ACS Chem. Biol. *8*, 741–748. http://dx.doi.org/10.1021/cb3006787.

Hur, S., and Bruice, T.C. (2003). The near attack conformation approach to the study of the chorismate to prephenate reaction. Proc. Natl. Acad. Sci. USA *100*, 12015–12020.

Karwowski, J.P., Jackson, M., Rasmussen, R.R., Humphrey, P.E., Poddig, J.B., Kohl, W.L., Scherr, M.H., Kadam, S., and McAlpine, J.B. (1993). 5-N-acetylardeemin, a novel heterocyclic compound which reverses multiple drug resistance in tumor cells. I. Taxonomy and fermentation of the producing organism and biological activity. J. Antibiot. *46*, 374–379.

Lee, C., Yang, W., and Parr, R.G. (1988). Development of the Colle-Salvetti correlation-energy formula into a functional of the electron density. Phys. Rev. B Condens. Matter *37*, 785–789.

Liesch, J.M., Hensens, O.D., Zink, D.L., and Goetz, M.A. (1988). Novel cholecystokinin antagonists from *Aspergillus alliaceus*. II. Structure determination of asperlicins B, C, D, and E. J. Antibiot. *41*, 878–881.

Linne, U., and Marahiel, M.A. (2004). Reactions catalyzed by mature and recombinant nonribosomal peptide synthetases. Methods Enzymol. *388*, 293–315.

Ma, S.M., Li, J.W., Choi, J.W., Zhou, H., Lee, K.K., Moorthie, V.A., Xie, X., Kealey, J.T., Da Silva, N.A., Vederas, J.C., and Tang, Y. (2009). Complete reconstitution of a highly reducing iterative polyketide synthase. Science *326*, 589–592.

Marenich, A.V., Cramer, C.J., and Truhlar, D.G. (2009). Universal solvation model based on solute electron density and on a continuum model of the solvent defined by the bulk dielectric constant and atomic surface tensions. J. Phys. Chem. B *113*, 6378–6396.

Merrick, J.P., Moran, D., and Radom, L. (2007). An evaluation of harmonic vibrational frequency scale factors. J. Phys. Chem. A *111*, 11683–11700.

Quadri, L.E.N., Weinreb, P.H., Lei, M., Nakano, M.M., Zuber, P., and Walsh, C.T. (1998). Characterization of Sfp, a *Bacillus subtilis* phosphopantetheinyl transferase for peptidyl carrier protein domains in peptide synthetases. Biochemistry *37*, 1585–1595.

Ribeiro, R.F., Marenich, A.V., Cramer, C.J., and Truhlar, D.G. (2011). Use of solution-phase vibrational frequencies in continuum models for the free energy of solvation. J. Phys. Chem. B *115*, 14556–14562.

Sanchez, J.F., Somoza, A.D., Keller, N.P., and Wang, C.C.C. (2012). Advances in *Aspergillus* secondary metabolite research in the post-genomic era. Nat. Prod. Rep. *29*, 351–371.

Sattely, E.S., Fischbach, M.A., and Walsh, C.T. (2008). Total biosynthesis: in vitro reconstitution of polyketide and nonribosomal peptide pathways. Nat. Prod. Rep. *25*, 757–793.

Takahashi, C., Matsushita, T., Doi, M., Minoura, K., Shingu, T., Kumeda, Y., and Numata, A. (1995). Fumiquinazolines A-G, novel metabolites of a fungus separated from a pseudolabrus marine fish. J. Chem. Soc. Perkin Trans. 1, 2345–2353.

Walsh, C.T., Haynes, S.W., and Ames, B.D. (2012). Aminobenzoates as building blocks for natural product assembly lines. Nat. Prod. Rep. *29*, 37–59.

Walsh, C.T., Haynes, S.W., Ames, B.D., Gao, X., and Tang, Y. (2013). Short pathways to complexity generation: fungal peptidyl alkaloid multicyclic scaffolds from anthranilate building blocks. ACS Chem. Biol., in press.

Yin, W.-B., Grundmann, A., Cheng, J., and Li, S.-M. (2009). Acetylaszonalenin biosynthesis in *Neosartorya fischeri*. Identification of the biosynthetic gene cluster by genomic mining and functional proof of the genes by biochemical investigation. J. Biol. Chem. *284*, 100–109.

